PHYSICAL REVIEW C VOLUME 36, NUMBER 6 DECEMBER 1987

Polarized, high-density, gaseous ^{3}He targets

T. E. Chupp and M. E. Wagshul
The Physics Laboratories, Harvard University, Cambridge, Massachusetts 02138

K. P. Coulter, A. B. McDonald, and W. Happer
Joseph Henry Laboratories of Physics, Princeton University, Princeton, New Jersey 08544

(Received 3 June 1987)

The technique of spin exchange between laser optically pumped alkali-metal vapor and ^{3}He can provide several atm cm^{-3} ($\approx 10^{21}$ atoms in a volume of 6 cm^3) of nearly 100% polarized ^{3}He. We have recently produced 40% polarization of 10^{20} atoms of ^{3}He (3 atm in 1.3 cm^3). It should therefore be possible to produce useful polarized ^{3}He targets by this technique. The realization of a practical target is limited by the contribution to depolarization by ionization during bombardment. This has been studied with a 360-nA, 18-MeV α-particle beam with encouraging results. A ^{3}He target with 50–90% polarization and a thickness of 10^{20} atoms cm^{-2} is feasible. This paper presents the principles of the technique, the recent progress on spin exchange with optically pumped alkali-metal vapor, and studies of ionization-induced depolarization.

I. INTRODUCTION

Polarized ^{3}He of density ($\approx 10^{21}$ atoms cm^{-3}) and polarization (50–90%) sufficient for a nuclear target can be produced by spin exchange with optically pumped Rb or K. Such a target has several exciting new applications including investigations of the quasielastic and Δ regions in polarized electron scattering and measurement of the electric form factor of the neutron,[1,2] study of nuclear parity violation[3,4] in ^{4}He and ^{19}Ne, and polarization and polarimetry of neutrons with energies[5] up to 10 eV for sensitive tests of parity and time reversal invariance in resonant neutron capture.[6,7] Since spin exchange is mediated by the hyperfine interaction of the alkali-metal electron with the ^{3}He nucleus during the 10^{-12}-s binary collision time, it is a very weak process. Carefully chosen target-cell wall materials and a high density of alkali-metal atoms are needed in order that the ^{3}He polarization rate be much greater than the wall relaxation rates. Contribution to relaxation of polarization due to ionization produced during bombardment must also be minimized.

We have studied the spin-exchange process, optical pumping of a high-density alkali vapor, and relaxation mechanisms. A polarized ^{3}He target has been constructed to study relaxation during bombardment with a 22-MeV α-particle beam. The results indicate that the target is practical for the electron scattering, parity violation, and polarized neutron studies. In this paper we present the results of these studies.

II. PRINCIPLES OF SPIN EXCHANGE

Polarization of ^{3}He follows from spin exchange due to the hyperfine interaction during binary collisions with electron-spin polarized alkali-metal atoms.[8–10] In this paper, spin exchange with Rb and K is discussed. For a completely polarized alkali-metal vapor [$\rho_A(+\frac{1}{2})=1$ where $\rho_A(\pm\frac{1}{2})$ is the occupation probability of $\pm\frac{1}{2}$ state of the alkali metal] the spin-exchange rate per atom of ^{3}He in the $m_K=-\frac{1}{2}$ state is

$$\gamma_{\rm SE}=\langle\sigma_{\rm SE}v\rangle[A]\ , \tag{1}$$

where $\langle\sigma_{\rm SE}v\rangle$ is the velocity-averaged rate constant, and $[A]$ is the alkali-metal number density. The rate constant has been measured for the ^{3}He-Rb system and given in Table I.

The rate equation governing the evolution of ^{3}He polarization is

$$\left[\frac{\Gamma}{2}+\gamma_{\rm SE}\rho_A(\tfrac{1}{2})\right]\rho(-\tfrac{1}{2})-\left[\frac{\Gamma}{2}+\gamma_{\rm SE}\rho_A(-\tfrac{1}{2})\right]\rho(+\tfrac{1}{2})=\frac{d}{dt}\rho(+\tfrac{1}{2})\ , \tag{2}$$

where $\rho(\pm\frac{1}{2})$ are the occupation probabilities for the $m_K=\pm\frac{1}{2}$ states in ^{3}He, and Γ is the relaxation rate for the ^{3}He polarization in the absence of alkali-metal vapor. The time evolution of the ^{3}He polarization, $P_3=\rho(+\frac{1}{2})-\rho(-\frac{1}{2})$, is given by

$$P_3=\frac{\gamma_{\rm SE}P_A}{\gamma_{\rm SE}+\Gamma}(1-e^{-(\gamma_{\rm SE}+\Gamma)t})\ , \tag{3}$$

where $P_A=\rho_A(+\frac{1}{2})-\rho_A(-\frac{1}{2})$ is the alkali-metal vapor's average polarization. The prescription for high polarization is clearly $\gamma_{\rm SE}\gg\Gamma$ and $P_A\approx 1$. We are currently able to polarize a density of [Rb]$\approx 10^{15}$ cm^{-3} in 1 cm^3 with $P_{\rm Rb}\approx 1$. In this case $\gamma_{\rm SE}=1/(2\ {\rm h})$. For a spherical cell of aluminosilicate glass, $\Gamma\approx 1/(40\ {\rm h})$, and an equilibrium polarization of 95% is expected.

The density and volume or equivalently the total number of ^{3}He atoms in the target are limited. The density is limited by two considerations: the pressure broadening of the $D1$ and $D2$ absorption lines in the alkali metal

TABLE I. Relevant constants for ^{3}He polarization.

	K	Rb
$D1$ wavelength	780 nm	795 nm
$D2$ wavelength	766.5 nm	770 nm
$\Delta\nu$ ($D1$-$D2$)	1780 GHz	7330 GHz
$\langle\sigma_{SE}v\rangle$ (A-^{3}He)		1.2×10^{-19} cm^3 s^{-1}
$\langle\sigma_{SD}v\rangle$ (A-A)	1.8×10^{-13} cm^3 s^{-1}	7.8×10^{-13} cm^3 s^{-1}

and the relaxation of the alkali-metal electron spin due to spin exchange with ^{3}He. The target volume is limited by the laser power available to keep the alkali-metal atoms polarized in the presence of relaxation. Pressure broadening and the limitations of laser power are discussed in more detail below.

III. LASER OPTICAL PUMPING OF HIGH-DENSITY ALKALI-METAL VAPOR

The principle of optical pumping is illustrated in Fig. 1 for an alkali metal, e.g., K or Rb for which $j=\frac{1}{2}$ in the ground state. In Fig. 1, the nuclear spin is neglected and the relevant states are the $s_{1/2}$ and $p_{1/2}$ states each with two magnetic substates $m_s=\pm\frac{1}{2}$. The nuclear spin introduces hyperfine splitting of 462 and 3036 MHz, respectively, for ^{39}K and ^{85}Rb. For our experiments, the laser linewidth far exceeds this splitting. Incident, circularly polarized light with magnetic projection $+1(\sigma_+)$ can only be absorbed by the $s_{1/2}$ state with $m_s=-\frac{1}{2}$. This populates the $p_{1/2}$ sublevel with $m_s=+\frac{1}{2}$ which decays to either sublevel of the ground state. In the absence of buffer-gas collisions which mix the two $p_{1/2}$ levels, the relative decay rates of the $p_{1/2}$ state with $m=+\frac{1}{2}$ are given by the Clebsch-Gordon coefficients, $\frac{2}{3}$ and $\frac{1}{3}$ as shown. However in a practical target, buffer-gas collisions randomize the p states and the relative decay rates to each sublevel of the ground state are $\frac{1}{2}$. As a result, two circularly polarized photons must be absorbed in order that a single unit of angular momentum is transferred to the atom. Furthermore, the $p_{1/2}$ states decay not only radiatively, but also nonradiatively through collisions with the buffer gas, specifically N_2.

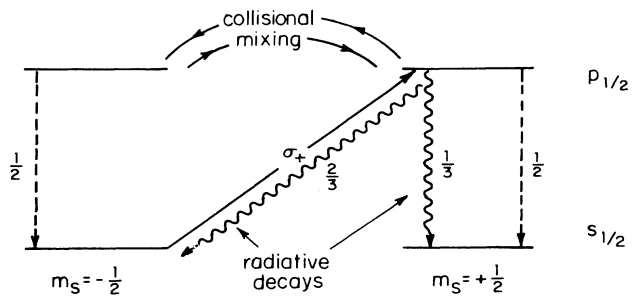

FIG. 1. Illustration of optical pumping with the nuclear spin neglected. The wavy lines correspond to no buffer gas and the dashed lines correspond to the presence of buffer gas.

As we shall discuss later, the radiative decay rates must be negligible compared to the nonradiative quenching rates.

An atom in the state $m_s=+\frac{1}{2}$ cannot absorb a σ_+ photon. Therefore as the vapor is optically pumped and the polarization grows, the vapor becomes transparent to the incident light.[11] The scattering length of the incident, right circularly polarized (σ_+) light of frequency ν is given by

$$\lambda^{-1}(\nu)=2[A]\sigma_{abs}(\nu)\rho_A(-\tfrac{1}{2}) , \tag{4}$$

where σ_{abs} is the cross section for scattering of unpolarized light, which depends on the total pressure in the cell and is about 10^{-12} cm^2 for this work. For $[A]\approx10^{15}$ cm^{-3}, λ is very short compared to 1 cm, the target dimension, unless the vapor is nearly polarized (i.e., $P_A>99.9\%$).

Within the high-density vapor the alkali-metal polarization is destroyed, predominantly by collisions with other alkali-metal atoms:[12,13]

$$A\uparrow+A\uparrow\rightarrow A\uparrow+A\downarrow . \tag{5}$$

This is probably due to a spin-spin interaction. The rate constants for spin destruction have been measured by Knize[13] and are given in Table I. In terms of this rate constant, the alkali-metal polarization relaxation rate is written

$$\Gamma_{SD}=\langle\sigma_{SD}v\rangle[A] . \tag{6}$$

The rate equation is

$$\left[\frac{\Gamma_{SD}}{2}+\gamma_{opt}\right]\rho_A(-\tfrac{1}{2})-\frac{\Gamma_{SD}}{2}\rho_A(+\tfrac{1}{2})=\frac{d}{dt}\rho_A(+\tfrac{1}{2}) . \tag{7}$$

Here γ_{opt} is the photon scattering rate *per alkali-metal atom* for an unpolarized vapor:

$$\gamma_{opt}=\int\Phi(\nu)\sigma_{abs}(\nu)d\nu , \tag{8}$$

where $\Phi(\nu)$ is the incident, circularly polarized photon flux (photons per unit area per unit time per unit frequency interval). The rate equation (7) has the equilibrium solution

$$P_A=\frac{\gamma_{opt}}{\gamma_{opt}+\Gamma_{SD}} . \tag{9}$$

The alkali-metal polarization will be nearly 100% as long as $\gamma_{opt}\gg\Gamma_{SD}$.

The flux $\Phi(\nu)$ and γ_{opt} for each alkali-metal atom depends on its position in the target because the incident, circularly polarized photons are scattered. The position dependence of $\Phi(\nu)$ is given by

$$\frac{d}{dx}\int \Phi(\nu)d\nu = -\int \lambda^{-1}(\nu)\Phi(\nu)d\nu$$

$$= -[A]\Gamma_{\text{SD}}P_A \ , \tag{10}$$

where x is the position in the cell along the direction of incidence. As long as $\gamma_{\text{opt}} \gg \Gamma_{\text{SD}}$ the integrated flux and γ_{opt} decrease linearly with x. At depths where the flux has decreased so that Γ_{SD} can no longer be neglected, $\Phi(\nu)$ and γ_{opt} will decrease exponentially with x and the alkali-metal polarization will rapidly fall to zero. The target can therefore be considered as two volumes, one in which the alkali-metal polarization is nearly 100% and the other in which it is nearly 0. The average polarization is the ratio of the 100% polarized volume ($V_{100\%}$) to the total volume. $V_{100\%}$ depends only on the laser power and the alkali-metal density:

$$\frac{P_{\text{total}}}{h\nu} = \Gamma_{\text{SD}}[A]V_{100\%}$$

and (11)

$$V_{100\%} = \frac{\dfrac{P_{\text{total}}}{h\nu}}{\langle \sigma_{\text{SD}} v \rangle [A]^2} \ ,$$

where P_{total} is the total laser power absorbed by the alkali-metal vapor in the target volume. Equation (11) predicts that 0.2 W/cm^3 of laser power be absorbed by the alkali-metal vapor for full Rb polarization at [Rb]$=10^{15}$ cm^{-3}. In the investigations described below, we have studied the laser power dependence of $V_{100\%}$ and the ^{3}He polarization rate and find reasonable agreement with this prediction.

The additional contribution to the spin destruction of the alkali metal can arise from interaction with the ^{3}He and N_2. At [Rb]$=10^{15}$ cm^{-3} the spin destruction due to Rb-Rb spin destruction is equal to that for Rb-^{3}He spin exchange when the ^{3}He pressure is 300 atm. The effect of about 100 Torr of N_2 appears to be negligible as indicated by Knize's work.[13] More detailed investigations are now underway. The total density of ^{3}He in the target is also limited by pressure broadening of the $D1$ and $D2$ resonance lines which overlap at about 100 atm for K and 400 atm for Rb. Pressures of 30 atm and [^{3}He]$=10^{21}$ cm^{-3} are therefore possible.

The phenomenon of radiation trapping can also limit effective optical pumping at high density. Radiation trapping is due to the radiative decay of the $p_{1/2}$ state, i.e., the scattering of the incident light which introduces unpolarized photons into the vapor. These unpolarized photons have a short scattering length, can be trapped within the vapor and will depolarize the alkali-metal atoms as they scatter. This can be accounted for by adding a decay term to the rate equation (7), and Eqs. (9)–(11) would be modified by replacing Γ_{SD} with $(\Gamma_{\text{SD}}+\alpha\gamma_{\text{opt}})$ where α is the ratio of unpolarized to polarized photons incident on each alkali-metal atom. As a consequence, if $\alpha\gamma_{\text{opt}}$ were not small relative to Γ_{SD} the vapor would not be polarized, the incident flux would fall off exponentially and the polarized atoms would be confined to a thin layer with thickness of order λ near the input wall. For the number densities appropriate to this work, $V_{100\%}$ would be independent of incident laser power and much less than 1 cm^3. This problem has been eliminated by insuring that the incident photons do not scatter, i.e., the $p_{1/2}$ state is nonradiatively quenched. Nonradiative quenching is effectively achieved with a modest pressure of N_2. Measurements by Hrycyshyn and Krause[14] indicate that the radiative and nonradiative quenching are equal at N_2 pressure of 3 Torr. In the investigations described below, 60–150 Torr of N_2 have been used and effective optical pumping has been achieved with no evidence of radiation trapping. This is shown by the observed dependence of the polarization rate on laser power. The possibility that less than 60 Torr of N_2 can effectively quench the $p_{1/2}$ states is under investigation.

IV. RESULTS OF RECENT EXPERIMENTS

We have produced 40% polarization of ^{3}He in a 1.3 cm^3 volume at a density of 10^{20} cm^{-3} by spin exchange with Rb. The spin-exchange rate constant[6] for Rb-^{3}He and the spin-destruction rate constants[13] have recently been measured. The dependence of ^{3}He polarization on laser power and alkali-metal density has been investigated and corroborates the expressions of Eqs. (3) and (11). The ^{3}He nuclear spin relaxation rate is affected by the choice of cell wall materials used, and aluminosilicate glass shows $\Gamma < 1/(40\text{ h})$. In this section, we describe these studies and the results.

The laser system used for this work consists of a Kr^+ ion laser which pumps a broadband standing-wave dye laser. The dye is LD700 which produces 2.0 W at 770 nm and 1.0 W at 795 nm, the $D1$ resonance wavelengths, respectively, of K and Rb. The multimode laser line width is specified as 40 GHz. The alkali-metal absorption linewidth is dominated by pressure broadening of the $p_{1/2}$ states which is 18 GHz/atm for Rb-He.[15] In our initial investigations, at total pressures of about 1 atm, less than the total incident laser power is absorbed by the cell. In more recent investigations, 3.5 atm samples are used which allowed greater efficiency for absorption of the laser power.

The ^{3}He is contained in a 1.5-cm diameter spherical glass cell. The cells are prepared by cleaning with water and methanol and evacuating to $<10^{-7}$ Torr while baking at 400 °C for at least 8 h. The alkali metal is then introduced into the cells by distillation with a flame. Varying pressures of ^{3}He and N_2 are mixed in the cell, and the cell is then pulled off forming a fused glass seal. For cells with total pressure greater than 1 atm at 300

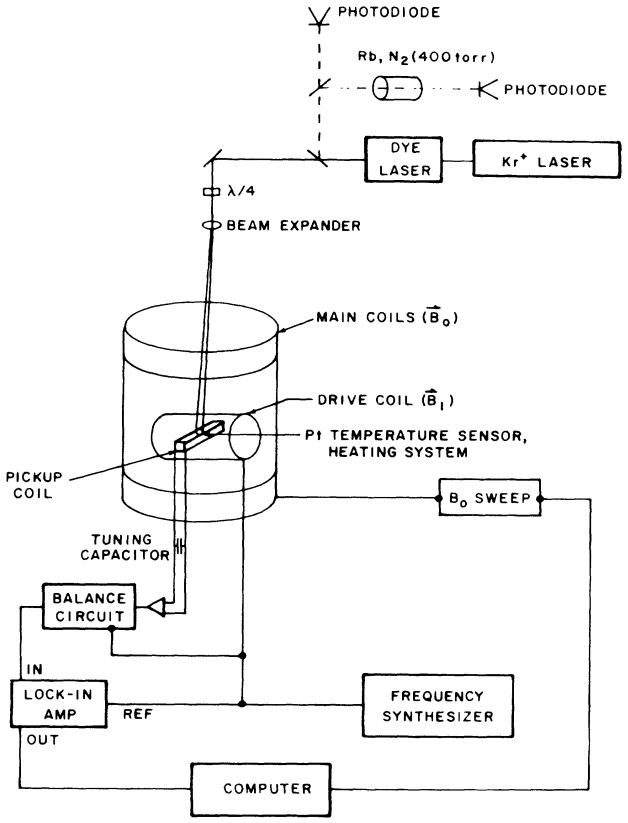

FIG. 2. NMR-AFP polarimeter. $\mathbf{B}_0$ corresponds to $\mathbf{B}_z$ and $\mathbf{B}_1$ to $\mathbf{B}_x$.

K, the pull-off procedure is executed at 77 K. Both borosilicate (Pyrex) and aluminosilicate (Corning 1720) glasses are used.

^{3}He polarization is measured with a NMR adiabatic-fast-passage[16] (AFP) polarimeter as illustrated in Fig. 2. The ^{3}He nuclei are polarized along the z axis. An oscillating magnetic field $[2\mathbf{B}_x \cos(\omega t)]$ is applied, typically 10-mG amplitude at 120 kHz. As the static field $\mathbf{B}_z$ is swept from below resonance to above and back down the nuclear magnetization follows the net field in the rotating frame: $\mathbf{B}_{\rm rot}=(B_z-\omega/\gamma)\hat{\mathbf{z}}+B_x\hat{\mathbf{x}}$, i.e., it flips from parallel to opposite $\mathbf{B}_z$ and back. The sweep rate, dB_z/dt is sufficiently slow to satisfy the adiabatic condition. During the process of flipping, the magnetization is precessing in the lab frame at the rate $\omega=2\pi\gamma\,|\,\mathbf{B}_z\,|$. The precessing magnetization induces a voltage in the pick-up coils oriented along the y axis,

$$V_0=\omega\Phi Q,\quad V_0=\omega\Phi Q\ , \tag{12}$$

where Φ is the flux through the pick-up coil's N turns and the coil forms part of a tuned circuit with quality factor Q. Φ can be accurately calculated for our geometry as the flux due to a uniformly magnetized sphere. The magnetization is [^{3}He] $P_3\mu_3$. In the regime of power broadening (B_x dominates the inhomogeneity of B_z across the cell) the AFP line shape as a function of $\Delta B=B_z-\omega/\gamma$ is given by

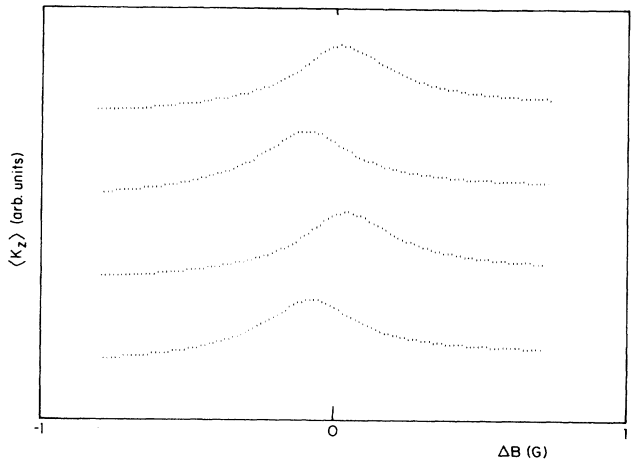

FIG. 3. A series of four NMR-AFP flips.

$$V(\Delta B)=V_0\frac{B_x}{(\Delta B^2+B_x^2)^{1/2}}\ . \tag{13}$$

The result of a series of four flips is shown in Fig. 3. This technique is particularly useful because it is nondestructive, i.e., the polarization can be probed and returned to its initial condition. This allows us to monitor the buildup and decay of polarization over several hours as illustrated by Fig. 4.

The ^{3}He polarization can be determined by fitting the line shape to the form of equation (13) and extracting P_3. The measurement is calibrated by measuring AFP signals from an identical cell filled with distilled H_2O where the density and polarization are known. The maximum observed ^{3}He polarization observed so far in our experiments is 40% after about 5-h pumping with Rb of density 6×10^{14} cm^{-3} in a Pyrex cell.

The spin exchange rate $\gamma_{\rm SE}$ is determined by pumping the vapor for several hours and then monitoring the decay of polarization with the laser off. As shown in Eq. (2), the decay of ^{3}He polarization with $P_A=0$ is

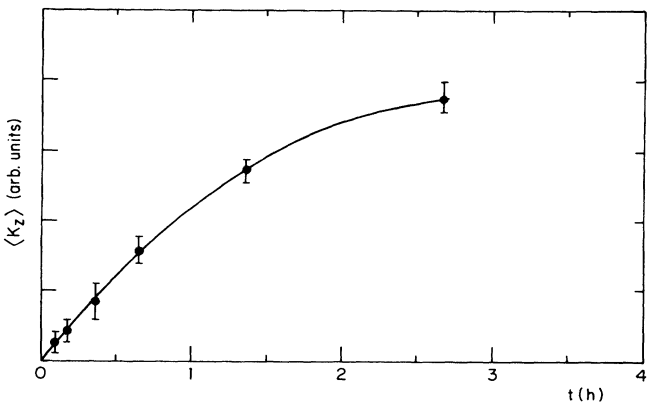

FIG. 4. The buildup of ^{3}He polarization over 3 h.

$$\frac{d}{dt}P_3 = -(\gamma_{SE}+\Gamma)P_3 \ . \tag{14}$$

The total decay rate of P_3 is linear in $[A]$ with slope $\langle \sigma_{SE} v \rangle$ and intercept Γ. These values are given in Table I. The alkali-vapor density-independent contribution to the relaxation rate is Γ. This includes contributions from dipole couplings near the cell walls and during collisions in the presence of magnetic field gradients. The wall relaxation rate is proportional to the sticking time of ^{3}He atoms at the cell wall. For borosilicate (Pyrex) glass, the sticking time is made effectively longer due to the diffusion of the atoms into the porous glass. Aluminosilicate glass (e.g., Corning 1720) is less porous to He and the sticking times are shorter. In our preliminary work with polarized ^{3}He, Pyrex cells were used and Γ was typically 1/(2 h). Our current aluminosilicate glass cells have Γ as small as 1/(40 h). The contribution to Γ due to magnetic field gradients is given by[9]

$$\Gamma = 0.47 \frac{\lambda v}{1+(\omega\tau_c)^2} \frac{\sum_{m=1}^{3} (\partial_m B_x)^2 + (\partial_m B_y)^2}{B_z^2} \ , \tag{15}$$

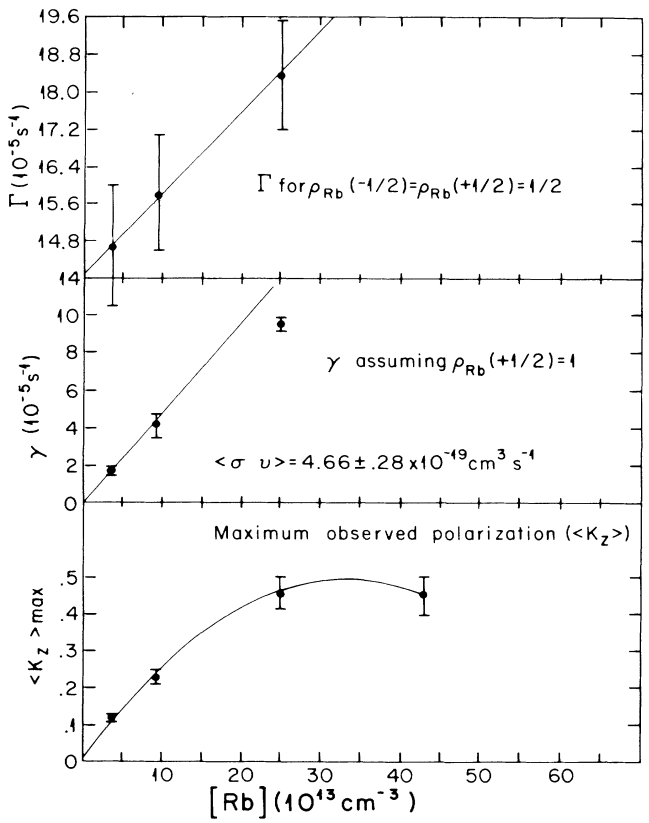

FIG. 5. Polarization of ^{21}Ne by spin exchange with Rb. Top: The decay rate of polarization with laser off. Γ is the *total* relaxation rate in this case. Middle: The polarization rate $\gamma_{SE}P_{Rb}$. Bottom: The maximum observed polarization as a function of [Rb].

where λ is the mean free path, v is the root mean square velocity, $\tau_c = \lambda/v$, and ω is the Larmor frequency. For a cell with ^{3}He density 10^{20} cm^{-3}, Γ is 1/(40 h) for a gradient of $6\times10^{-3}B_z$ cm^{-1}.

The dependence of polarization rate (dP_3/dt) and maximum observed polarization has been investigated with the Rb-^{21}Ne system.[10] In this work the Rb probably absorbed 0.1 W of laser power. As illustrated in Fig. 5, the polarization rate and polarization rise linearly with [Rb] up to about 3×10^{14} cm^{-3}. Beyond this density, the fall off is due to the decrease of $V_{100\%}$ to less than the cell volume as predicted by Eq. (11).

The dependence of polarization rate on laser power has been studied with the Rb-^{3}He system. In this case, total power ranging from 0.1 to 0.5 W was incident on the cell at densities of 3.4 and 6.5×10^{14} cm^{-3}. The results are displayed in Fig. 6. For laser power insufficient to pump the cell (i.e., below about 0.4 W for the lower Rb density) the polarization rate rises linearly with laser power and saturates as $V_{100\%}$ becomes larger than the cell's volume. Furthermore, in the region of linear dependence on laser power, the slope is inversely proportional to $[Rb]^2$ as predicted in Eq. (11). With sufficient laser power to pump the entire cell volume, the polarization rates are linear with [Rb].

The total volume of polarized Rb has also been measured in a large cell with 3 atm of ^{3}He and 200 Torr of N_2 at $[Rb]=10^{15}$ cm^{-3}. The scattered $D2$ fluoresence light is used to define the region into which the light penetrates. For 0.12 W of power incident on the alkali-metal vapor, $V_{100\%}$ is observed to be 0.3 cm^3. This is in agreement with the data shown in Fig. 6 and the prediction of Eq. (11).

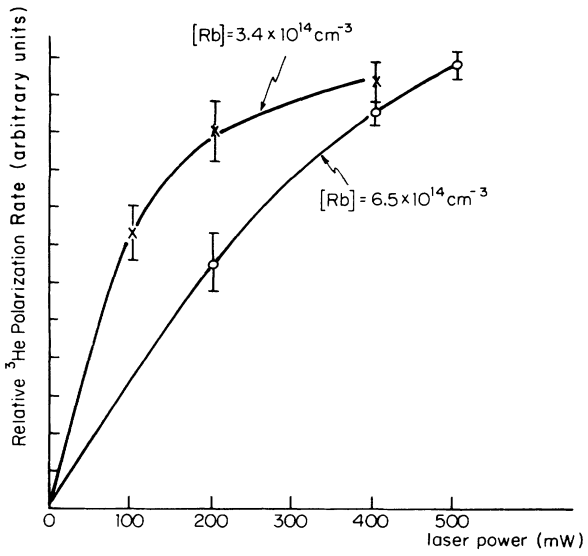

FIG. 6. The dependence of polarization rate on the laser power exiting the laser for Rb-^{3}He with $[Rb]=3.4$ and 6.5×10^{14} cm^{-3}. The solid lines are provided as a visual guide.

V. RELAXATION OF POLARIZATION DURING BOMBARDMENT

The experiments described above were performed in closed glass cells, not during bombardment by an accelerator beam. During bombardment there exist addition contributions to the ^{3}He depolarization rate Γ which are proportional to the rate, per ^{3}He atom, at which the ^{3}He ions are produced by the incident beam. As discussed in detail by Bonin, Walker, and Happer,[17] the depolarization rate depends on the total pressure in the target, the presence of N_2 and other species including impurities and on the magnetic field. As shown below, targets that will be produced by spin exchange can have a small ionization contribution to Γ. This is due to the N_2 and the high total pressure of several atmospheres. A measurement performed at the Princeton Cyclotron confirms this.[23] Work reported by Milner, McKeown, and Woodward[18] is also in progress at Caltech with targets of high purity ^{3}He at low pressure.

The contribution to Γ due to ionization can be written as

$$n_d \Gamma_i = (n_a + n_m)\Gamma_i \ , \tag{16}$$

where Γ_i is the mean ionization rate per atom of ^{3}He defined by

$$\Gamma_i = \left[\frac{dE}{dx}\right]^{\mathrm{He}} \frac{1}{E_{\mathrm{ion}}^{\mathrm{He}}} \frac{L}{V} i_b \ . \tag{17}$$

Here V is the target volume, i_b is the beam current in particles per second, $(dE/dx)^{\mathrm{He}}$ is the energy loss per incident beam particle per ^{3}He atom per cm^2, $E_{\mathrm{ion}}^{\mathrm{He}} \approx 32$ eV is the mean energy required to produce an ion pair from a target atom, and $L[^3\mathrm{He}]$ is the target thickness of ^{3}He in atoms cm^{-2}. The number of ^{3}He atoms that are depolarized for each atom ionized, n_d, can vary from zero to many thousands. n_a characterizes the contribution to Γ due to the ^{3}He$^+$ atomic ions produced, and n_m characterizes the contribution due to the formation of molecular ions ^{3}He$_2^+$.

The atomic depolarization number n_a will have a value between 0 and 1, depending on the magnetic field and on the partial pressures of ^{3}He, of N_2, and of various impurity gases. Each newly formed ^{3}He$^+$ ion has a probability of $\frac{1}{2}$ of being in the state with the electron and nuclear spins antiparallel. In this state the hyperfine interaction $A\mathbf{S}\cdot\mathbf{K}$ can transfer nuclear spin polarization $\langle K_z \rangle$ to the polarization $\langle S_z \rangle$ of the unpaired electron of the ^{3}He$^+$ ion. The angular momentum transfer will be interrupted by ^{3}He$^+$-^{3}He charge exchange collisions, and the unpaired electron will be transferred to a "fresh" nucleus from which it can extract more angular momentum. These collisions can occur repeatedly until the ion is destroyed which may be sufficiently long for the angular momentum of the unpaired electron to saturate, that is, $\langle S_z \rangle = \langle K_z \rangle$. There will be no further nuclear spin depolarization after saturation. This limiting situation corresponds to $n_a = 1$. For the conditions of the measurements described here, we expect $n_a \approx \frac{1}{2}$, since too few ^{3}He$^+$-^{3}He charge exchange collisions can occur, before the ^{3}He$^+$ ion is destroyed by a charge exchange collision with a N_2 molecule.

The ^{3}He$^+$ ions can also form ^{3}He$_2^+$ molecular ions. The molecular ions contribute to ^{3}He depolarization by atom exchange with polarized atoms and spin-rotation coupling in the molecule. As we show below, under the conditions in a target produced by spin exchange, this contribution to Γ is negligible for two reasons: the depolarization rate within the molecular ion is small at high pressures and the N_2 destroys the molecular ions.

The contribution to the depolarization rate Γ due to collisions of the polarized ^{3}He atoms with molecular ions is

$$n_m \Gamma_i = k_m \int [^3\mathrm{He}_2^+] \frac{dV}{V} \ , \tag{18}$$

where k_m is the rate constant for depolarization of ^{3}He. The volume integral reflects the fact that the ions may not occupy the entire target volume since the incident beam will generally not fill the volume and the ions may be quickly destroyed. k_m is estimated to be $\approx 10^{-12}$ cm^3 s^{-1} at 20 Torr on the basis of experimental work by Byerly.[19] For target pressures above a critical pressure, estimated in Ref. 17 to be about 10 Torr, the time between atom collisions is too short to permit complete nuclear depolarization in the ^{3}He$_2^+$ molecular ion. For target pressures much less than the critical pressure, the rate constant k_m is independent of pressure. For target pressures much greater than the critical pressure, the regime in which our work is carried out, the rate constant k_m should be inversely proportional to the square of the total pressure in the target.

The density of molecular ions is determined by the balance of production and destruction rates. The atomic ions produced can be neutralized by charge exchange with N_2 or form molecular ions in three body collisions. The balance of the production and destruction rates for ^{3}He$^+$ gives

$$\Gamma_i [^3\mathrm{He}] V = (\alpha_{\mathrm{N}} [\mathrm{N}_2] + \beta_{\mathrm{He}} [^3\mathrm{He}]^2) \int [^3\mathrm{He}^+] dV \ , \tag{19}$$

where $\alpha_{\mathrm{N}} = 10^{-9}$ cm^3 s^{-1} and $\beta_{\mathrm{He}} = 10^{-31}$ cm^6 s^{-1}. The first term[20] on the right-hand side is the rate for charge exchange with N_2, and the second term[21] is the rate for molecular ion formation by three body collisions.

In our experiments, the destruction of molecular ions[22] is dominated by charge transfer to N_2. The rate per molecular ion for this process is $k[\mathrm{N}_2]$ where $k = 6 \times 10^{-10}$ cm^3 s^{-1}. Several other species (Ne, H_2O, H_2, etc.) are also effective in charge transfer destruction of the ^{3}He$_2^+$ molecular ions. The equilibrium density of ^{3}He$_2^+$ ions is determined by the balance of the destruction and production rates,

$$k[\mathrm{N}_2] \int [^3\mathrm{He}_2^+] dV = \beta_{\mathrm{He}} [^3\mathrm{He}]^2 \int [^3\mathrm{He}^+] dV \ . \tag{20}$$

Combining Eqs. (18), (19), and (20) we find the molecular depolarization number to be

$$n_m = \frac{k_m}{k} \frac{[^3\mathrm{He}]^3}{(\alpha_{\mathrm{N}}/\beta_{\mathrm{He}})[\mathrm{N}_2]^2 + [^3\mathrm{He}]^2 [\mathrm{N}_2]} \ . \tag{21}$$

In the measurement described below a target with 430 Torr ^{3}He and 150 Torr N_2 was used. Scaling Byerly's[19] 20 Torr value of k_m by the square of the ratio of pressures, $(20/580)^2$, we find $k_m \approx 1.2\times10^{-15}$ cm^{-3}s^{-1} for our conditions. Equation (21) predicts $n_m = 3\times10^{-8}$.

Investigations are currently underway at the Princeton Cyclotron to measure depolarization rates of ^{3}He during bombardment. Preliminary results[23] have been obtained with a 360 nA beam of 18 MeV alpha particles incident on a target with 430 Torr of ^{3}He and 150 Torr of N_2 in a volume of approximately 1 cm^3. The contribution to Γ due to ionization is $\approx 1/(3$ h), and $n_d \leq 1$. The ionization rate due to the 400 nA beam of 22 MeV alpha particles is equivalent to that of a 10 μA beam of 400 MeV electrons.

The problem of depolarization during bombardment is also being studied at Caltech[18] where a target with 1–6 Torr of polarized ^{3}He is produced by metastability exchange with optically pumped metastable ^{3}He. For their work $n_d \approx 1800$. This large value of n_d is consistent with a dominant contribution to the depolarization due to $^3He_2^+$ molecular ions and a negligible contribution from the atomic ions $^3He^+$, that is, $n_d \approx n_m \gg 1$. The tightly bound molecular ions, once formed, can be destroyed only by slow diffusion to the container walls or by charge exchange collisions against impurity gases such as H_2O or N_2 which may have been present in the Caltech target.[17]

For the targets discussed in this paper, the high density of N_2 molecules destroys most of the atomic ions before they can be converted to molecular ions, and the few molecular ions which do form are destroyed by charge exchange collisions with N_2 molecules before they have a chance to cause significant depolarization. The small value of n_d observed in these is consistent with a dominant contribution from the atomic ions and negligible contribution from the molecular ions, that is, $n_d \approx n_a < 1$.

VI. SUMMARY: FUTURE PROGRESS AND PROMISE

We have shown that up to 90% polarization of $>10^{20}$ atoms of ^{3}He in a 6-cm^3 volume can be produced by spin exchange. Up to 10^{21} atoms cm^{-3} can be polarized with currently available laser power. With more laser power, higher densities and greater polarization rates or larger volumes can be polarized. The use of K in place of Rb may be favorable because the spin-destruction rate constant is 5 times less for K, and the LD700 dye produces about 2 times more power at 770 nm, the K $D1$ line than at 795 nm, the Rb $D1$ line. However the K-^{3}He spin-exchange cross section has not yet been measured. Studies of depolarization during bombardment show that a high-density target produced by the spin-exchange technique has a relaxation rate of $1/(3$ h) for 400 nA of 22-MeV alpha particles, consistent with our model.

The luminosity possible with 10 μA of 400-MeV polarized electrons incident on the target can be 10^{33} cm^{2}s^{-1} with about 50–90% steady polarization. This target can have a thickness of 10^{20} cm^{-2} of ^{3}He and 5×10^{18} cm^{-2} of N_2 which is needed to quench radiation trapping and aid three-body recombination of $^3He_2^+$ ions. As shown in Ref. 6, with 90% polarized ^{3}He at a pressure of 8 atm ($[^3He]=2.1\times10^{20}$ cm^{-3}) in a 1.2×5 cm^3 volume, neutron polarization of 1.0 with transmission 0.45 at 0.025 eV and polarization of 0.6 with transmission 0.65 at 1 eV are possible with ^{3}He polarization of 90%. The analyzing power for polarized neutrons is equal to the polarization at each energy. The ^{3}He polarization in a target can be reversed at a rate greater than 1 s^{-1} which allows the study of systematic effects which are an important consideration in the proposed neutron electric form factor and parity and time reversal violation experiments.

We are currently investigating the possible utilization of new laser technologies. Two new types of laser are promising. The alexandrite laser recently developed by Allied Chemical works best as a pulsed device. High repetition rates (100 Hz–1 kHz) seem possible and may be appropriate for optical pumping. The requirement is that the alkali-metal spin-destruction rate be small compared to the laser repetition rate. These lasers are unfortunately expensive but could provide 50 W average power. It is therefore not likely that alexandrite lasers will lead the way to the first polarized targets.

GaAs diode lasers work very well at the longer wavelengths including 795 nm. Single mode, monolithic diodes produce up to 20 mW with a bandwidth of $\sim$1 MHz. Striped arrays of diode lasers which are gain coupled are now being produced, but these are not single mode devices, i.e., each element of the array can lase in a different mode. Recently however, the elements of an array have been mode locked to a master single mode laser.[24] This is a very promising technology which should be considered for polarized targets. In particular it should prove less expensive than the current scheme involving the Kr^+-dye laser combination.

ACKNOWLEDGMENTS

We wish to gratefully acknowledge discussions with A. Bernstein, K. Bonin, T. Walker, R. Milner, R. McKeown, D. Tieger, and E. D. Earle. This material is based upon work supported by a National Bureau of Standards Precision Measurement Grant, a grant from the Research Corporation and the National Science Foundation under Grants Phy-8605081 and Phy-8604510. T.E.C. acknowledges additional support from the Afred P. Sloan Foundation.

[1]A. M. Bernstein, in *Workshop on Polarized ^{3}He Beams and Targets*, Proceedings of the Conference on Polarized ^{3}He Beams and Targets, AIP Conf. Proc. No. 131, edited by R. W. Dunford and F. P. Calaprice (AIP, New York, 1985), p. 165.

[2]B. Blankleider and R. M. Woloshyn, Phys. Rev. C **29**, 538 (1984).

[3]T. E. Chupp, W. Happer, and A. B. McDonald, in Proceed-

ings of the Workshop on Polarized Targets in Storage Rings, [Argonne National Laboratory Report No. ANL-84-50, 1984 (unpublished), p. 177].
[4]A. B. McDonald, Bull. Am. Phys. Soc. **31**, 1196 (1986).
[5]W. G. Williams, Nukleonika **25**, 769 (1980).
[6]K. P. Coulter, A. B. McDonald, W. Happer, T. E. Chupp, and M. E. Wagshul, in *Proceedings of the Workshop on Time Reversal Invariance in Neutron Physics, Chapel Hill, 1987* (World-Scientific, Singapore, 1987).
[7]J. D. Bowman, C. D. Bowman, and V. Yuan, in *Proceedings of the Workshop on Time Reversal Invariance in Neutron Physics,* Ref. 6.
[8]M. A. Bouchiat, T. R. Carver, and C. M. Varnum., Phys. Rev. Lett. **5**, 373 (1960).
[9]R. L. Gamblin and T. R. Carver, Phys. Rev. **138**, A964 (1965).
[10]T. E. Chupp and K. P. Coulter, Phys. Rev. Lett. **55**, 1074 (1985).
[11]N. D. Bhaskar, M. Hou, B. Suleman, and W. Happer, Phys. Rev. Lett. **43**, 519 (1979).
[12]N. D. Bhaskar, J. Pietras, J. Comparo, W. Happer, and J. Miron, Phys. Rev. Lett., **44**, 930 (1980).
[13]R. Knize (private communication).
[14]E. S. Hrycyshyn and L. Krause, Can. J. Phys. **48**, 2761 (1970).
[15]S-Y Che'en and M. Takeo, Rev. Mod. Phys. **29**, 20 (1957).
[16]A. Abragham, *Principles of Nuclear Magnetism* (Oxford University Press, CITY, 1961) pp. 34–36.
[17]K. Bonin, T. Walker, W. Happer, to be published.
[18]R. G. Millner, R. D. McKeown, and C. E. Woodward, NIM in Phys. Res. **A257**, 286 (1987).
[19]R. Byerly, Jr., Ph. D. thesis, Rice University, 1967 (unpublished).
[20]J. Heimerl, R. Johnsen, and M. A. Biondi, J. Chem. Phys. **51**, 5041 (1969).
[21]Massey, *Electronic and Ionic Impact Phenomena* (Oxford University Press, London, 1981).
[22]D. K. Bohme, N. G. Adams, M. Moseman, D. B. Dunkin, and E. F. Ferguson, J. Chem. Phys. **52**, 5094 (1970).
[23]K. P. Coulter, A. B. McDonald, G. Cates, and T. E. Chupp (unpublished).
[24]L. Goldberg *et al.* Appl. Phys. Lett., **46**(3) 236 (1985).